Experimental and Computational Study of the Zn_nS_n and $Zn_nS_n^+$ Clusters

Andrei Burnin, Edward Sanville, and Joseph J. BelBruno*

Center for Nanomaterials Research and Department of Chemistry, Dartmouth College, Hanover, New Hampshire 03755

Received: February 7, 2005; In Final Form: March 29, 2005

Zinc sulfide clusters produced by direct laser ablation and analyzed in a time-of-flight mass-spectrometer, showed evidence that clusters composed of 3, 6, and 13 monomer units were ultrastable. The geometry and energies of neutral and positively charged Zn_nS_n clusters, up to $n = 16$, were obtained computationally at the B3LYP/6-311+G* level of theory with the assistance of an algorithm to generate all possible structures having predefined constraints. Small neutral and positive clusters were found to have planar geometries, neutral three-dimensional clusters have the geometry of closed-cage polyhedra, and cationic three-dimensional clusters have structures with a pair of two-coordinated atoms. Physical properties of the clusters as a function of size are reported. The relative stability of the positive stoichiometric clusters provides a thermodynamic rationale for the experimental results.

Introduction

ZnS is an important wide band gap ($E_g = 3.65$ eV) II−VI semiconductor, which can be used in the fabrication of optoelectronic devices such as blue or UV light emitting diodes,[1] laser diodes,[2] *n*-window layers in solar cell technology,[3] and emissive flat screens.[4] By their nature, clusters represent the link between an ensemble of separate atoms or molecules and a bulk material. The spatial evolution from atomic to bulk states through the variety of sizes and configurations results in a dramatic change of properties, which are of particular fundamental and technological interest. As the number of particles constituting a cluster increases, the configuration space of available cluster isomers grows significantly. Some clusters exhibit exceptional stability relative to neighboring sizes. Those correspond to "magic number clusters", whose stability, in general, may be conferred either by geometric or electronic considerations. Despite considerable theoretical effort,[5−9] the zinc−sulfur system remains not fully understood with respect to the relative stability of the clusters as revealed from experiment.

The time-of-flight mass spectrometry (TOF−MS) study of ZnS clusters, obtained by laser ablation of solid zinc sulfide followed by a helium gas quench of the vapor, was reported by Martin[10] and later, using direct laser ablation of zinc sulfide or mixtures of elemental precursors, from our group.[11] Theoretically, small neutral stoichiometric Zn_nS_n clusters ($n = 1-9$) were described using density functional theory.[5] The authors concluded that $(ZnS)_2$ four-membered rings and $(ZnS)_3$ six-membered rings were the pertinent building blocks for larger three-dimensional structures. This idea was extended in a comparative theoretical study of the relative stability of hollow cage or bubble neutral clusters[6,7] vs bulklike crystallites for clusters up to $n = 47$. Recent advances in structure prediction led to the use of a genetic algorithm[9] to predict the geometries of neutral clusters of up to 15 monomer units. The largest structures, $n = 240$, were investigated using Hartree−Fock molecular orbital calculations.[8] The authors used lattice translational symmetry to reduce the number of two-electron integrals and to compute the properties of the clusters as crystallites. The $Zn_nS_n^+$ clusters have not been previously studied. Here, we focus on the relationship of the cluster structures to their physical properties and to the laser ablation mass spectrum.

Experimental Details

Zinc−sulfur clusters were generated in a time-of-flight mass spectrometer equipped with a Nd:YAG laser as described previously.[11] The materials used for cluster production included 99.995% pure zinc sulfide powder (Strem Chemicals) or mixtures of 99.95% pure elemental zinc (Fisher Scientific) and 99.95% pure sulfur (Mallinckrodt) powders. Molar ratios of zinc to sulfur were chosen to be 1:1, 2:1 and 1:2. In the ablation process, the high-voltage pulses were applied to the accelerator after a delay time of either 60 or 80 μs to record mass-spectra of smaller and larger clusters, respectively.

Computational Details

Since the topological trend for neutral clusters was understood from preliminary ab initio calculations and the literature, a search algorithm was applied to scan through the entire space, searching for a connectivity matrix representing a cluster with a particular bonding topology. In addition, particularly for zinc sulfide 13-mer geometries, a genetic algorithm developed to study MgO clusters,[12] was applied with suitable pair interaction potentials for ZnS.[11]

All final optimizations, neutral and cationic, were performed with NWChem, a Computational Chemistry Package for Parallel Computers, Version 4.5.[13,14] The correlation and exchange effects were calculated at the B3LYP level of theory[15,16] with the 6-311+G* basis set both for sulfur[17,18] and zinc[19,20] atoms. Single-point calculations at the same level of theory were performed on positively charged clusters having the optimized geometries of the neutral clusters in order to locate the vertical ionization energies. All calculations were run in parallel on a Beowulf Linux cluster comprised of 20 IBM x335 nodes (40 2.8 GHz Xeon CPUs) with 50 GB of memory and 2 TB of disk space. Geometric structures of zinc−sulfur clusters and their molecular orbitals were visualized using *Chem 3D Pro 8.0*.[21]

10.1021/jp050657c CCC: $30.25
Published on Web 05/18/2005

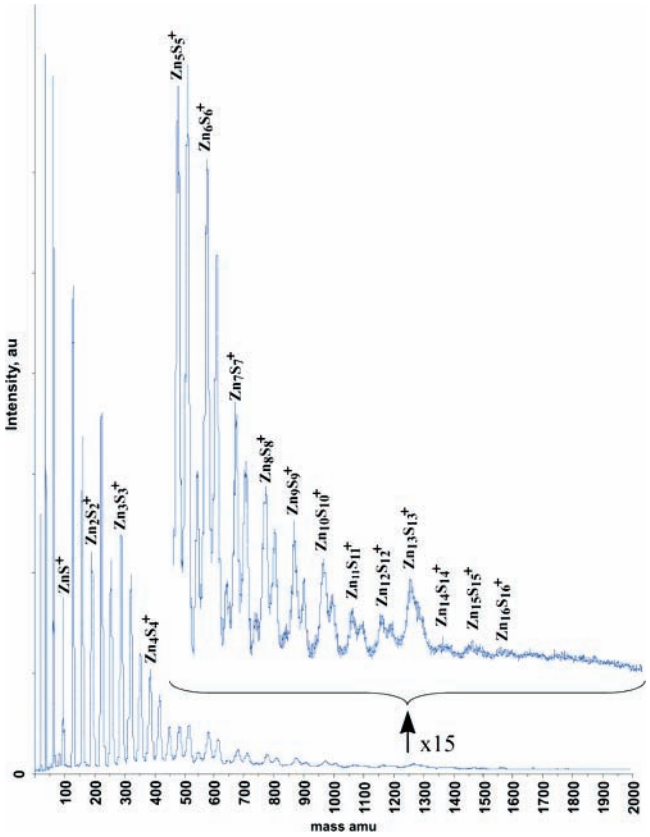

Figure 1. Mass spectrum of ZnS clusters obtained by direct ZnS laser ablation.

Results and Discussion

Mass Spectra. The mass spectrum obtained by laser ablation of solid ZnS is shown in Figure 1. Nearly identical ZnS cluster spectra were obtained using various molar ratio mixtures of zinc and sulfur powders. Because the peak intensities fit a log−normal distribution and decrease quickly as a function of the number of monomer units, the large mass region is presented in the inset where intensities are multiplied by a factor of 15. The signals correspond to the masses of three different classes of clusters: $Zn_nS_n^+$, $Zn_nS_{n+1}^+$ and $Zn_{n+1}S_n^+$. Peak broadening is caused by the overlap of unresolved signals from cluster isotopomers composed of the following major isotopes (and percent abundances):[22] ^{64}Zn (48.63), ^{66}Zn (27.90), ^{67}Zn (4.10), and ^{68}Zn (18.75); ^{32}S (94.93) and ^{34}S (4.29).

Computational Results: Neutral Clusters. Almost all of the neutral clusters and several cluster cations take on structures predicted by Euler's theorem, which provides the relationship among the number of faces, vertexes, and edges, in any simple, closed polyhedron. This rule allows one to determine the number of four- and six-membered rings, N_4 and N_6 respectively, for any Zn_nS_n structure. The use of the theorem yields $N_4 = 6$; the number of four-membered rings in Zn_nS_n is fixed for all closed structures. In addition, this provides that the number of six-membered rings is given by $N_6 = n - 4$, where n is the total number of monomer units. The structures of the neutral clusters have received attention from several research groups.[5−10] With a single exception ($n = 7$), our calculated geometries for the neutral clusters of up to nine monomer units agree with those reported by Matxain et al.[5] Beginning at $n = 6$, these structures are those that would be predicted from Euler's theorem for closed polyhedra. Figure 2 presents the neutral global minimum structures for clusters with $1 \leq n \leq 16$. Selected local minima are presented in Figure 3. Since the main points regarding the geometries of the neutral clusters have already been reported, only issues relevant to our subsequent discussion are presented. However, all of the structures are shown.

The tetramer is the last planar minimum energy structure, in agreement with the literature.[5] The S−Zn−S angle is close to 180°. The zinc atom sp hybridization in the bonding with sulfur, which contributes unhybridized p orbitals, leads to Zn−S−Zn angles of 93.4°. The local minimum tetramer cage geometry, **4a**, shown in Figure 3, is the first possible Euler structure and is constructed from four-membered ring building blocks. All Zn−S bond lengths in this conformer are 2.380 Å. The S−Zn−S and Zn−S−Zn bond angles are 105.1 and 72.4°, respectively. The angles are indicative of the ring strain, leading to an energy 1.10 eV above the global minimum.

Our calculations indicate that the hexamer, **6**, previously reported as the global minimum,[5] has the lowest energy *only* if diffuse Gaussian basis functions are included in the large triple-ζ basis set. This is the first molecule to contain only three-coordinated atoms in its global minimum configuration. There were several interesting local minima detected. One, **6a** in Figure 3 and 0.55 eV above the global minimum, preserves the cyclic configuration, resembling a chair-structure containing S−Zn−S angles of 178.3°, Zn−S−Zn angles of 97.9°, and Zn−S bond length of 2.180 Å.

The Zn_7S_7 cluster is the only neutral molecule for which our results are in disagreement with previous calculations.[5] Our results, at a higher level of theory, predict the Euler's theorem structure, **7** in Figure 2, to be more stable. This geometry has three six-membered rings and includes two sets of three adjacent four-membered rings built from bonds in the length range 2.292−2.371 Å. Shown in Figure 3, structure **7a** is the previously reported 7-mer structure, now located 0.25 eV above the global minimum.

The global minimum Zn_8S_8 cluster takes on an Euler structure.[5] A series of other geometries were analyzed, including a prism and a ring. A twisted octagonal prism, **8a** in Figure 3, is a local minimum. Because of the presence of two eight-membered rings, the number of six-membered rings in this structure is zero and the number of four-membered rings increases from six to eight. The large number of adjacent four-membered rings sharing bonds should render the structure less energetically favorable than **8**, however inexplicably, the energy difference between this geometry and the global minimum (0.03 eV) is insignificant. All bond lengths within the eight-membered rings are 2.282 Å and the distance between the rings is 2.496 Å.

The minimum energy structures for $Zn_{10}S_{10}$ and $Zn_{11}S_{11}$ satisfy Euler's theorem. The $Zn_{12}S_{12}$ cluster, **12**, is the first structure that permits the separation of all four-membered rings. For this polyhedron, Euler's theorem requires eight six-membered rings. There are only two bond types in this structure.[6] One is shared by two six-membered rings, 2.269 Å, and the second is shared by a six-membered ring and a four-membered ring, 2.352 Å. The search algorithm revealed another interesting structure, **12a** in Figure 3. The distortion from **12** increases the energy by 1.03 eV, because of the increased strain in the two sets of adjacent four-membered rings. Bond lengths are 2.254−2.367 Å.

The lowest energy $Zn_{13}S_{13}$ structure, **13** in Figure 2, is the Euler structure reported by Spano et al.[6] This structure, with bond lengths in the 2.266−2.392 Å range, has no symmetry. Our group,[11] has previously reported two other structures obtained from a genetic algorithm.[12] These are local minima,

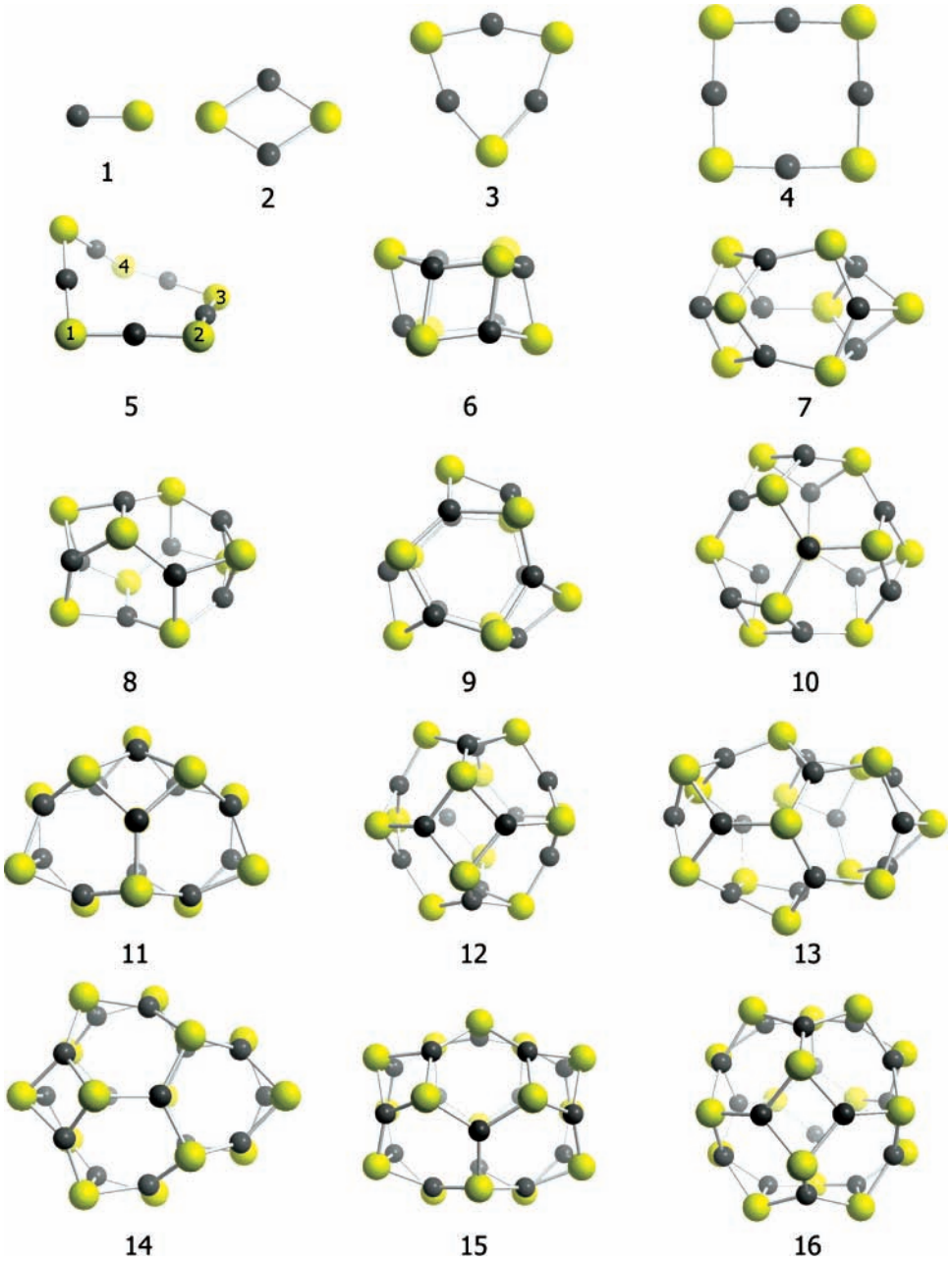

Figure 2. Geometric structures of global minima neutral Zn_nS_n clusters ($n = 1-16$). Dark spheres are zinc atoms and light spheres are sulfur atoms.

higher in energy by ~0.21 eV. One such structure, **13a** in Figure 3, has a single eight-membered ring, which requires one additional four-membered ring. The other previously reported structure, **13b** in Figure 3, may be easily envisioned as the global minimum 12-mer with a monomer unit inserted in place of a bond linking two four-membered rings. The bond length range, 2.143−2.376 Å, is rather broad. Euler's theorem predicts a third structure,[11] which was obtained from a fragment of the wurzite lattice, **13c** in Figure 3. The structure has three sets of adjacent four-membered rings, which makes it energetically less favorable. This geometry is 0.49 eV above the global minimum. Because the global minimum structure has two sets of two adjacent four-membered rings and **13c** has three such sets, the difference in total energy of 0.49 eV may be attributed to an increase arising from the additional set of adjacent four-membered rings.

The number of sets of adjacent four-membered rings in the global minimum 14-mer, **14** in Figure 2, is one. This was confirmed by an exhaustive examination of possible Euler's theorem structures using our search algorithm. It has six four-membered rings and 10 six-membered rings, and the bond lengths span the 2.262−2.402 Å range. We also examined another structure obtained from the search algorithm programmed to seek structures with two sets of adjacent four-membered rings, structure **14a** in Figure 3. Its bond lengths lie in the range 2.249−2.391 Å. The energy difference between these two structures, 0.51 eV, may be attributed to the increase arising from the additional pair of adjacent four-membered rings in **14a**. The minimum energy $Zn_{15}S_{15}$ cluster geometry is an Euler structure. For the 16-mer, the search algorithm returned two structures with all six four-membered rings isolated. The global minimum structure, **16**, is symmetric and bond lengths are in a narrow range, 2.300−2.334 Å. The next lowest energy structure, **16a** in Figure 3, also has all four-membered rings separated, but it is located 0.14 eV above the T_d structure and has bond lengths in the range, 2.253−2.351 Å.

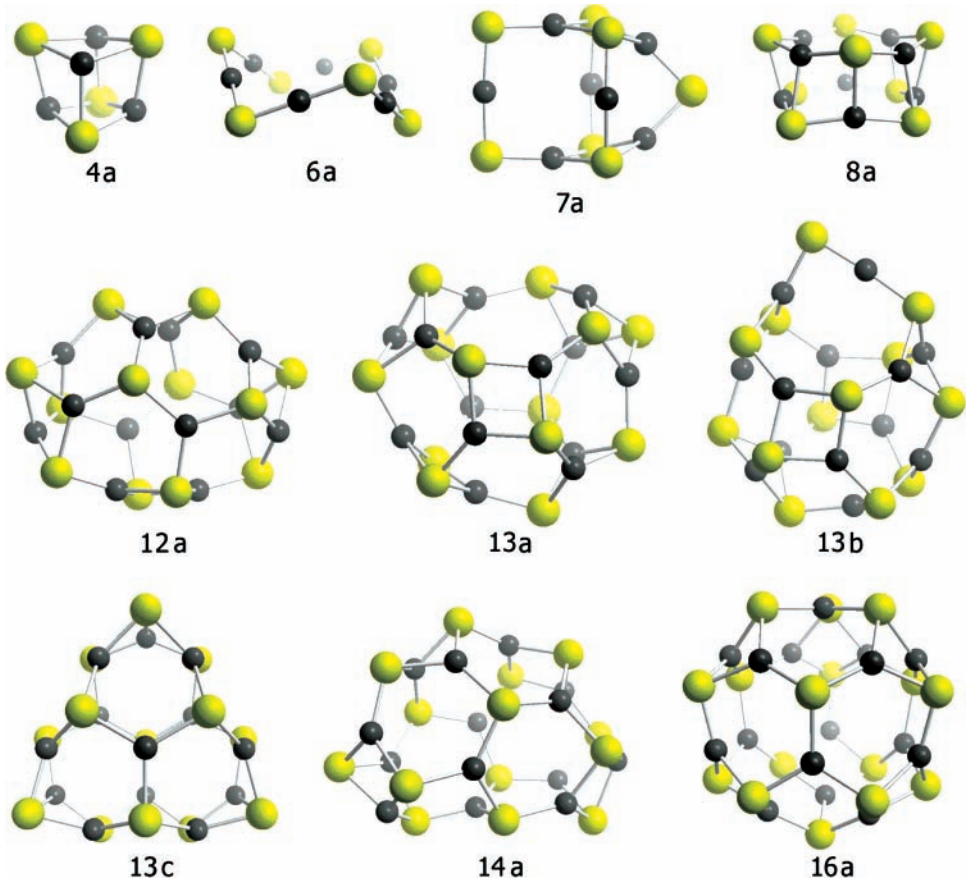

Figure 3. Geometric structures of selected local minima neutral Zn_nS_n clusters. The structures are labeled by the number of monomer units. Dark spheres are zinc atoms and light spheres are sulfur atoms.

Computational Results: Positively Charged Clusters. The optimized geometries of the global minimum cationic clusters ($n = 1-16$) are shown in Figure 4. In the figure, clusters are labeled according to the number of monomer units and the cationic nature is indicated by +. The first five cationic clusters have the same symmetry as their corresponding neutral clusters. Bond lengths and bond angles, of course, take on different values. Bond lengths, in particular, are longer since the electron is removed from an orbital with at least partial bonding character. Beginning with $Zn_6S_6^+$, two-coordinated atoms appear in the global minimum structures and geometries in agreement with Euler's theorem become local minima. The cationic cluster structures have not been previously reported. They are described in detail below.

The positive monomer, $\mathbf{1}^+$, has a 2.185 Å bond length, which is 0.102 Å longer than in the neutral molecule. As in the neutral dimer, the positive global minimum structure, $\mathbf{2}^+$, is a rhomboid. Here, all bond lengths are 2.278 Å and S−Zn−S angles, 109.9°. In comparison with the neutral structure, the positive dimer has 0.148 Å longer bonds. The positive global minimum trimer, $\mathbf{3}^+$, is planar and has slight variations in the bond lengths, over the range 2.186−2.240 Å, similar to the neutral trimer.

In the $Zn_4S_4^+$ global minimum, $\mathbf{4}^+$, all Zn−S bond lengths are 2.190 Å, which is longer than in the neutral cluster of the same geometry. The S−Zn−S angles are 174.1° and Zn−S−Zn angles 95.9°. The S−Zn−S angles are approximately 176.0°, and the Zn−S bond lengths lie in the 2.170−2.205 Å range for $Zn_5S_5^+$, $\mathbf{5}^+$. The dihedral angle of the rectangular part of the geometry, S(1)−S(2)−S(3)−S(4), is 8.0°, indicating a larger distortion than in the neutral pentamer, which has the same overall geometry.

Beginning with the hexamer cation, the global minimum structures include two-coordinated atoms in preference to Euler structures. The shape of $\mathbf{6}^+$ is similar to that of the neutral cluster, **6**, except in the cation, two adjacent four-membered rings have been replaced by a six-membered ring. The bond lengths are 2.209−2.451 Å and the Zn−S−Zn and S−Zn−S angles at the two-coordinated atoms are 91.1 and 151.4°, respectively. The structure that satisfies Euler's theorem is a local minimum, 0.24 eV higher in energy. In the global minimum heptamer cation, $\mathbf{7}^+$, bond lengths fall in the range 2.190−2.467 Å. At the two-coordinated atoms, the Zn−S−Zn and S−Zn−S angles are 85.0 and 153.0°, respectively. The Euler polyhedron is 0.59 eV higher in energy. $Zn_8S_8^+$, $\mathbf{8}^+$, has bond lengths in the range 2.185−2.474 Å. The Zn−S−Zn angle at the two-coordinated sulfur atom is 87.9° and the angle at the two-coordinated zinc atom is 157.1°. The Euler structure is located 0.13 eV above this global minimum. The global minimum positive 9-mer, $\mathbf{9}^+$, continues the trend of including two-coordinated atoms. The bond lengths range from 2.186 to 2.428 Å. The angles at the two-coordinated sulfur and zinc are 87.1 and 154.5°, respectively. A local minimum Euler structure is 0.39 eV above the global minimum. The minimum energy $Zn_{10}S_{10}^+$ structure, $\mathbf{10}^+$, has bond lengths in the 2.181−2.419 Å range, and angles at the two-coordinated sulfur and zinc atoms are 86.7 and 156.0°, respectively. The Euler structure is located 0.86 eV above the global minimum. For the $Zn_{11}S_{11}^+$, global minimum, $\mathbf{11}^+$, bond lengths fall in the range 2.179−2.436 Å. The angles at the two-coordinated atoms are 85.6 and 155.4°, for sulfur and zinc. A number of local minima, including that predicted by Euler's theorem (0.37 eV) are located 0.20−0.93 eV above the global minimum.

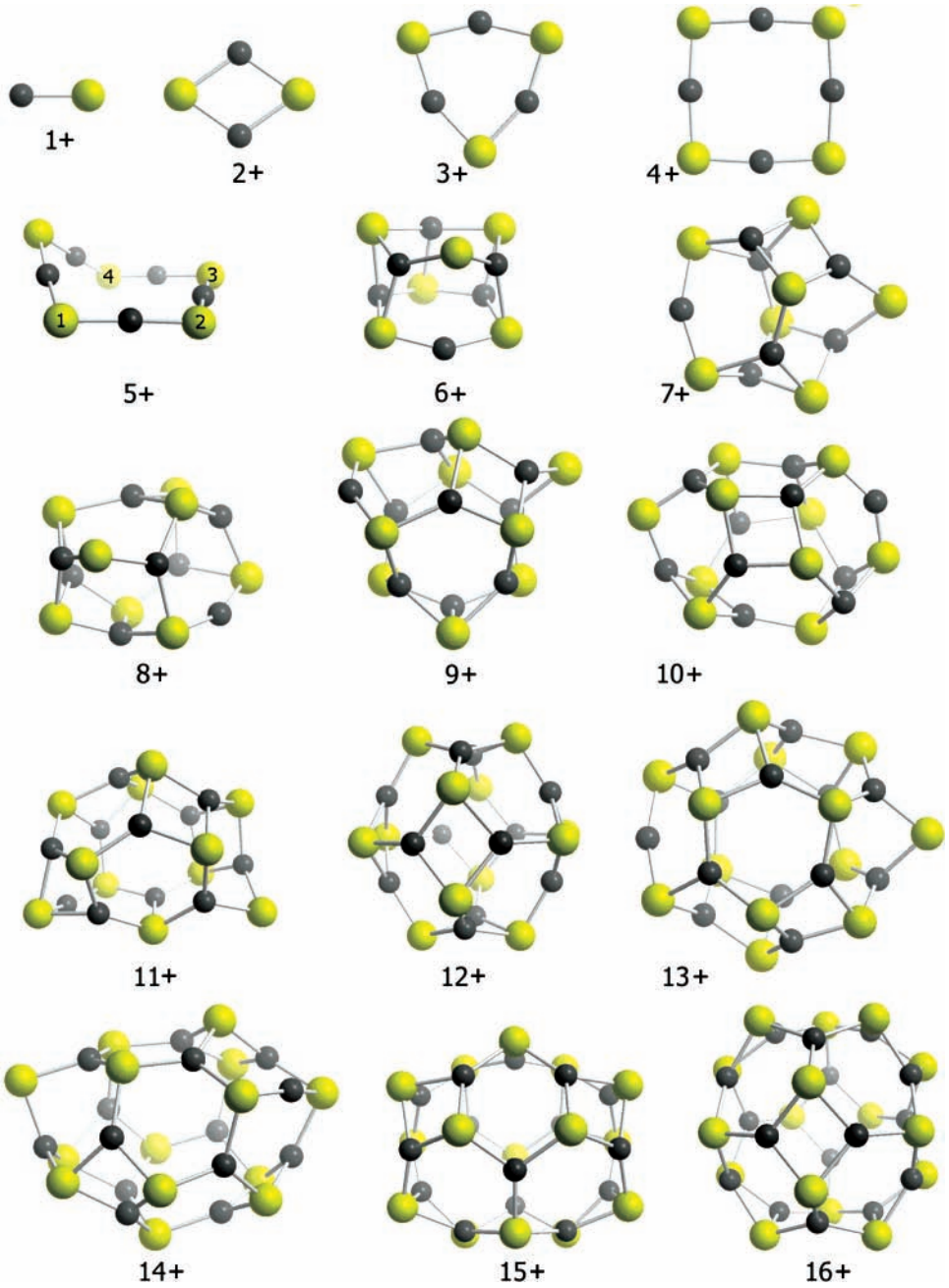

Figure 4. Geometric structures for the global minima $Zn_nS_n^+$ clusters from monomer to 16-mer. Dark spheres represent zinc atoms and light spheres are sulfur atoms.

Remarkably, the 12-mer, $\mathbf{12}^+$, is the first cation structure where the global minimum is represented by the Euler topology, as it was for the neutral cluster. The bond lengths range from 2.245 to 2.359 Å. Fourteen other 12-mer structures with two-coordinated atoms were tested. The most stable of these structures is located only 0.10 eV above $\mathbf{12}^+$. The global minimum 13-mer, $\mathbf{13}^+$, reverts back to the two-coordinated atom topology. Bond lengths lie in the range 2.206−2.402 Å and angles at the two-coordinated atoms are 87.8 and 161.5° for sulfur and zinc, respectively. Local minima with two-coordinated atoms are 0.07−0.17 eV higher in energy. The structure consistent with Euler's theorem lies much (0.64 eV) higher. The 14-mer cation cluster global minimum, $\mathbf{14}^+$, also includes two-coordinated atoms. The bond length interval is 2.197−2.381 Å, the angle at the two-coordinated sulfur is 87.7° and that at the two-coordinated zinc is 160.2°. Nine other local minima structures, plus the Euler's theorem structure, 0.26 eV above the global minimum, were examined. Global minimum structures return to those consistent with Euler's theorem for the final positive clusters, $\mathbf{15}^+$ and $\mathbf{16}^+$. The bond lengths lie in the range 2.235−2.389 and 2.251−2.388 Å, respectively. In the case of the 15-mer, 17 other local minima structures with two-coordinated atoms were analyzed. One such structure is situated only 0.02 eV above the global minimum. Twenty-two local minimum 16-mer structures with two-coordinated atoms were found.

Cluster Structure. The ultimate goal of the calculations is an attempt to rationalize the relative stability of ZnS clusters reflected in the mass spectrum in Figure 1: is the experimental data reflective of neutral or cationic cluster geometry? Previous research has shown that, depending on the target, the mass spectrum may be dominated by either the relative stability of neutral species[23,24] or cationic clusters.[25] In both situations, the relative stability of clusters is generally considered to derive

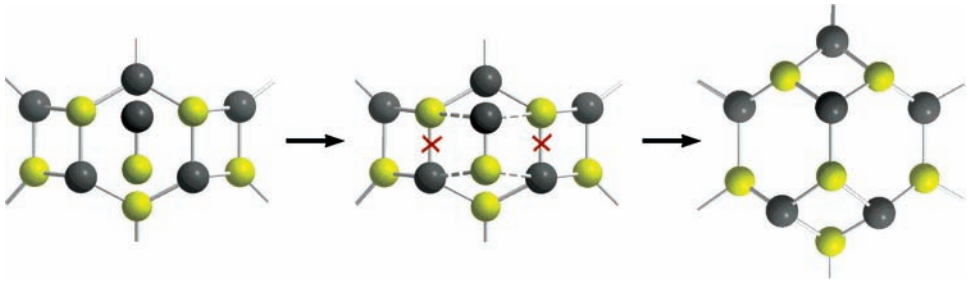

Figure 5. Insertion of monomer unit in the transition from Zn_nS_n to $Zn_{n+1}S_{n+1}$.

from their electronic or geometric structures. There are two competitive configuration choices for the overall geometry of the zinc sulfide clusters: crystallites, as in alkali metal halide clusters, or cages, as in carbon fullerenes. This is determined by a compromise between ionic vs covalent interactions in bond formation. Ionic bonds are isotropic, while covalent bonds are directional. Thus, in the case of large covalent contributions to bonding, ionic close-packing might be dominated by the tendency to form bonds in a preferred direction. In the cage clusters, all of the cations and anions were three-coordinated; this configuration is intermediate between the two-coordinated states in small clusters and the four-coordinated situation in the bulk. The structures reported here do not reflect crystallite geometries. Clearly, the cluster bonding is anisotropic, indicating that the overall charge separation in the clusters is small.

From the computational results, one may conclude that the zinc sulfide clusters are similar to fullerenes, which are constructed from pentagons and hexagons, where $N_5 = 12$ and $N_6 = (n - 20)/2$. The addition of a single seven-membered ring to a fullerene requires an additional pentagon and reduces the number of hexagons by two[26] to compensate for the negative curvature. This topological parallel between zinc sulfide clusters and fullerenes may be made even more explicit. It is known that fullerenic structures are more stable if the number of isolated pentagons is maximized. Kroto formulated this as the isolated pentagon rule.[27] The smallest possible fullerene, C_{20}, constructed only from pentagons, as a dodecahedron, is extremely unstable.[28] For the neutral clusters, Zn_4S_4, the first possible Euler structure, **4a**, is not a global minimum. Thus, analogous to the isolated pentagon rule for fullerenes, the isolated tetragon rule may be established for ZnS clusters and, presumably, extended as the isolated lowest order polygon rule for any closed-cage polyhedron topology of clusters. As for zinc sulfide clusters, it is possible to support this rule quantitatively by comparing the energies of *n*-mer isomers with different numbers of sets of adjacent four-membered rings. Thus, ΔE_{adj}, the energy increase (ring strain) due to a set of adjacent rings, is

$$\Delta E_{adj} = \frac{E(n,m) - E(n,k)}{m - k} \qquad (1)$$

Here, $E(n,m)$ and $E(n,k)$ are the energies of *n*-mers with different numbers, *m* and *k*, of sets of adjacent four-membered rings. For the neutral clusters, there are three such possibilities: (1) 12-mers, **12** and **12a**, (2) 13-mers, **13** and **13c**, and (3) 14-mers, **14** and **14a**. For these three cases, the energy increase due to the addition of one set of adjacent four-membered rings, ΔE_{adj}, is nearly identical: 0.52, 0.49, and 0.51 eV, respectively. We conclude that two adjacent four-membered rings introduce a ring strain, which would be relieved by relaxation to a single six-membered ring. However, this rearrangement is constrained by other bonding interactions, including the energy increase due to the presence of two-coordinated atoms, so that the neutral clusters maintain the structure that satisfies Euler's theorem. Clearly, such constraints do not exist for the cation clusters.

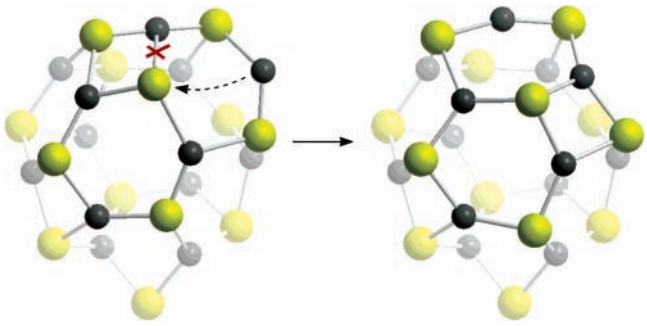

Figure 6. Reconfiguration of the positive 13-mer cluster due to the shift of a zinc atom.

Another parallel to the fullerenes was observed; for a given neutral *n*-mer, the neighboring $n+1$ Euler structure may be obtained by insertion of a ZnS monomer unit to a six-membered ring. The monomer should be inserted inverse-parallel to two bonds shared by a six-membered ring and each four-membered ring. These two bonds are broken and four new bonds are formed as illustrated in Figure 5. The procedure is similar to the insertion of a C_2 dimer into a fullerene molecule.[27]

For the cationic clusters, small, $n \leq 5$, molecules retain the geometry of the neutrals, except that all Zn−S bonds are elongated relative to those in the corresponding neutral clusters. This can be considered the result of the removal of an electron from a bonding HOMO and the need to accommodate the charge. For larger positive clusters, there are significant changes in topology. In the Euler hexamer, ionization causes a bond to break, leading to structure $\mathbf{6}^+$, Figure 4. This introduction of two-coordinated atoms reduces the number of four-membered rings to four and reduces ring strain due to adjacent four-membered rings. The presence of two-coordinated atoms in the cationic clusters increases the energy by ∼25 kJ/mol, but elimination of a four-membered ring adjacency, decreases the energy by 50 kJ/mol. Thus, the net gain is ∼25 kJ/mol. The presence of two-coordinated atoms provides additional geometric flexibility as outlined in Figure 6. A two-coordinated zinc atom forms a new bond to a sulfur atom shared by six- and four-membered rings, while a second bond breaks in a concerted process, causing migration of the two-coordinated atom over the surface. Reconfiguration from a strained Euler structure to one with two-coordinated atoms appears to be facile. The barrier for the shift of the zinc atom was found using a relaxed potential energy scan procedure. The barrier is approximately 1 kJ/mol. For Euler structures without such adjacent rings, two-coordinated atoms are not needed and are detrimental to the structure. This is what was observed for the positively charged 12-, 15-, and 16-mers. In all of these cases, no structure involving two-coordinated atoms is energetically preferable to a structure that satisfies Euler's theorem.

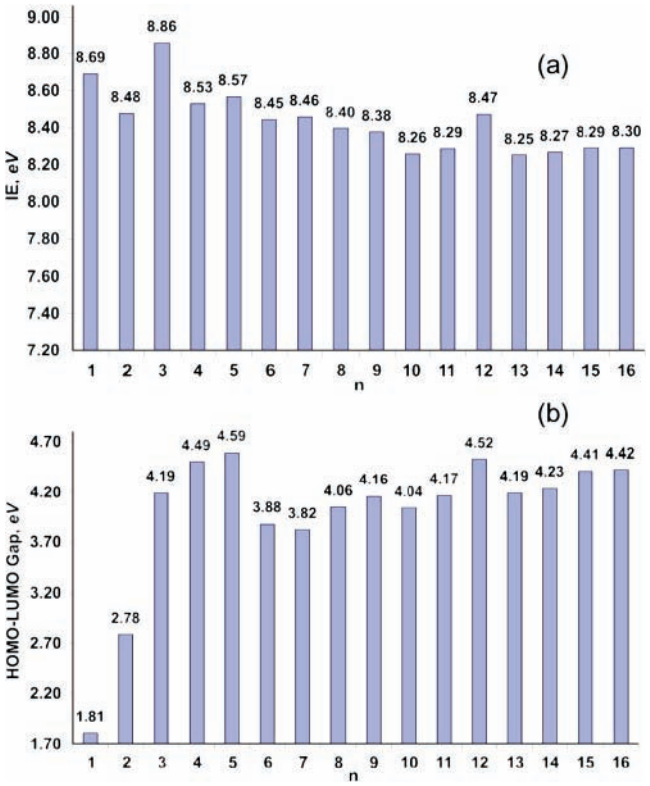

Figure 7. Properties of Zn_nS_n clusters: (a) vertical ionization energy and (b) HOMO−LUMO gap.

Cluster Properties. We now turn to the properties of the clusters as a function of size. The neutral zinc sulfide cluster-structures are used to extract the information. For example, the vertical ionization energy of each cluster was calculated as the energy difference between the cation having the geometry of the corresponding neutral cluster and the neutral cluster itself, Figure 7a. The large ionization energies of the trimer and the 12-mer arise, within the concept of Koopmans' theorem, due to the low lying HOMOs for the neutral clusters relative to those of their $n \pm 1$ neighbors. The HOMO−LUMO energy gap is presented in Figure 7b. Examination of the relevant molecular orbitals indicates that the gap is controlled by the position of the LUMO for small ($n \leq 5$) clusters, while for Euler structures, the energy of the HOMO is the major variable. The bulk comparison point for the HOMO−LUMO separation is the band gap for ZnS in the zinc blende form, $E_g = 3.65$ eV. Comparison of this parameter with the HOMO−LUMO gap of larger clusters indicates that over the course of the clusters studied, the gaps increase to a value greater than the band gap. DFT calculations are known to overestimate the HOMO−LUMO gap in semiconductors. Despite the fact that the shapes of some of the structures are far from spherical, several cluster properties may be plotted as a function of $1/\sqrt[3]{n}$, a quantity proportional to the inverse of the *effective* cluster radius. The value from such a plot extrapolated to zero, corresponds to the bulk parameter. Figure 8a depicts the best linear fit and the intercept for the atomization (cohesive) energy per monomer unit for the three-dimensional structures ($n = 6-16$). Extrapolation predicts the bulk atomization energy to be 574 ± 20 kJ/mol, which is in excellent agreement with the experimental value 607 kJ/mol.[28] Similarly, the extrapolation of cluster ionization energy to infinity, Figure 8b, returns the photoelectric threshold for bulk zinc sulfide, 7.71 ± 0.35 eV, in agreement with the experimental value, 7.60 ± 0.30 eV, obtained from photoemission experiments.[29] These results are surprising because the structures used for both extrapolations correspond to cages rather than the small

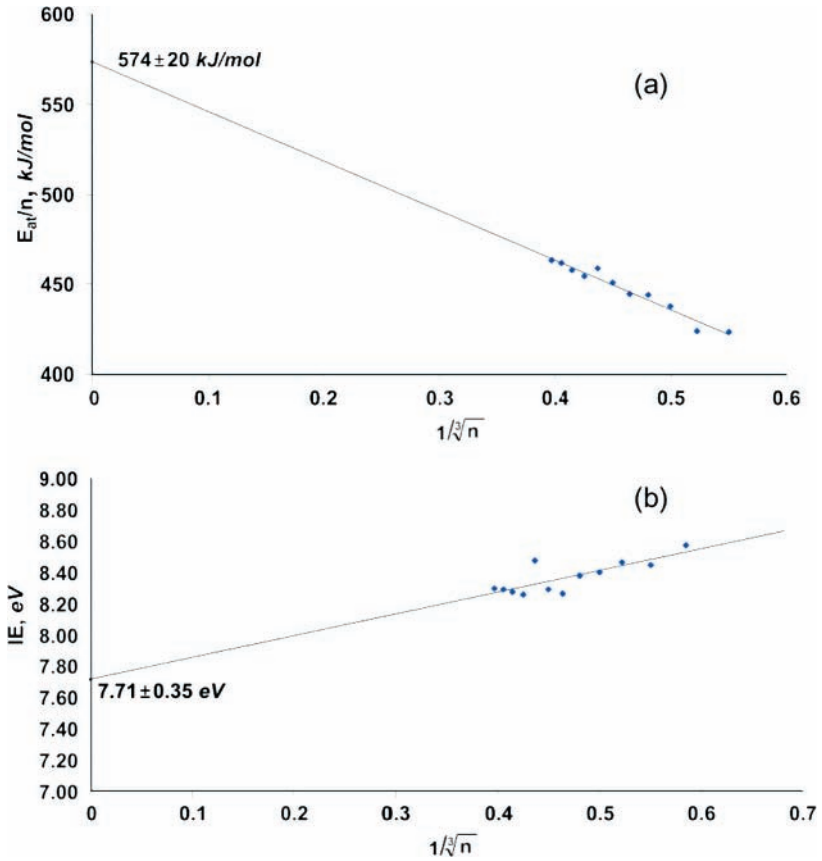

Figure 8. Extrapolation of (a) atomization energy and (b) ionization energy of clusters to bulk.

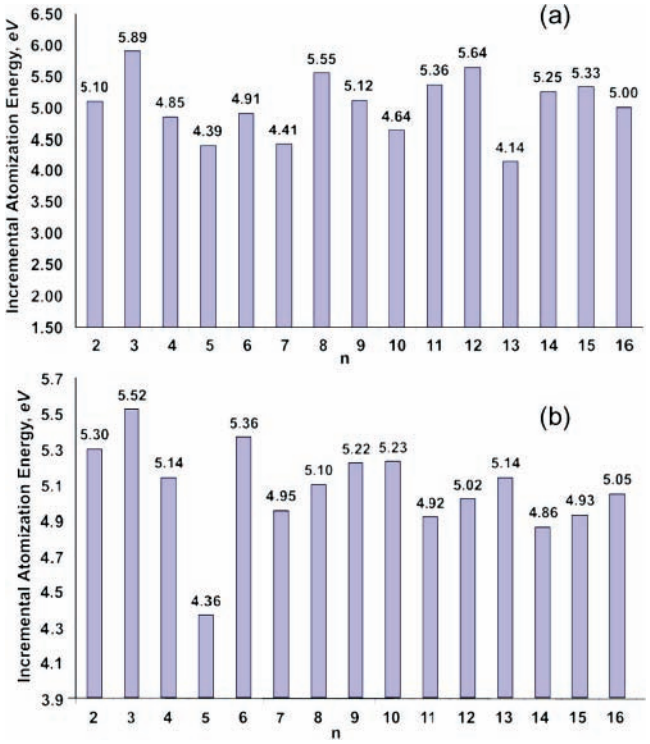

Figure 9. Incremental atomization energy of (a) Zn_nS_n and (b) $Zn_nS_n^+$ clusters.

crystalline clusters representing the zinc blende or wurzite lattice at a small scale.

Mass Spectrum/Structure Correlation. The question of the structural basis for the observed ultrastable clusters in the mass spectra remains. One often-employed measure of structural stability is the incremental atomization energy. This is defined for neutral clusters as

$$\Delta E_{at}(n) = E_{at}(n) - E_{at}(n-1) \quad \text{or}$$
$$\Delta E_{at}(n) = E(n-1) + E(\text{Zn}) + E(\text{S}) - E(n) \quad (2)$$

where $E_{at}(n)$ is the atomization energy and $E(n)$ is the total energy of an n-mer cluster. That is, we calculate the energy required for the hypothetical detachment of zinc and sulfur atoms from the n-mer to form an $n-1$ predecessor

$$Zn_nS_n \rightarrow Zn_{n-1}S_{n-1} + Zn + S \quad (3)$$

The dependence of $\Delta E_{at}(n)$ on the number of clustering monomer units is shown in Figure 9a. Comparison of the relative column heights in the figure with the relative peak intensities in the mass spectrum, Figure 1, indicates that the latter are not reflective of the incremental atomization energies of the neutral species. Thus, the examination of relative stability of positive clusters is necessary. The incremental atomization energy of the positive clusters is defined in the analogous manner. Now, the incremental energy reflects the energy necessary to eject zinc and sulfur atoms from a positive n-mer to form a cationic $(n-1)$-mer in the reaction

$$Zn_nS_n^+ \rightarrow Zn_{n-1}S_{n-1}^+ + Zn + S \quad (4)$$

The dependence of the incremental atomization energy on the number of clustering monomer units, n, is shown in Figure 9b. There is nearly exact agreement between the relative stability indicated by the mass-spectrum, Figure 1, and the relative stability estimated from the incremental atomization energy of the positive zinc sulfide clusters. The magic numbers 3, 6, and 13 are in agreement, as are the relatively low stabilities of the $n = 5$, 7, 11, and 14 positive clusters. Clearly, the mass spectrum reflects the direct formation of ions within the ablation plume. Modeling[30] has indicated that this is the preferential channel for cluster formation under these experimental conditions. Clusters are seeded by ions, which then polarize nearby neutral atoms and molecules. These molecules then play the role of building material for the cluster.

Summary

Zinc sulfide clusters were produced in a laser ablation source, time-of-flight mass-spectrometer. The mass spectrum indicated that clusters composed of 3, 6, and 13 monomer units were ultrastable. In a parallel study, the geometries and energies of neutral and positively charged Zn_nS_n clusters up to $n = 16$ were obtained computationally. Small neutral and positive clusters ($n \leq 5$) have planar geometries, while neutral three-dimensional clusters have the geometry predicted by Euler's theorem for closed-cage polyhedra with all atoms in a three-coordinated state. Cationic three-dimensional clusters, on the other hand, have cage structures with a pair of two-coordinated atoms, unless separation of adjacent four-membered rings is not necessary for stability. The HOMO−LUMO gap and ionization energies of the neutral clusters were shown to trend toward the known bulk parameters, the band gap and cohesive energy, with increasing cluster size. The relative stability of the positive stoichiometric clusters expressed in terms of the incremental atomization energy vs the number of clustering monomer units provides a thermodynamic explanation for the relative stability observed in the laser ablation of zinc sulfide.

References and Notes

(1) Mauch, R. H. *Appl. Surf. Sci.* **1996**, 589.
(2) Iida, S.; Sugimoto, T.; Suzuki, S.; Kishimoto, S.; Yagi, Y. *J. Cryst. Growth* **1985**, *72*, 51.
(3) Ndukwe, I. C. *Solar Energy Mater. Solar Cells* **1996**, *40*, 123.
(4) Leskela, M. *J. Alloys Compd.* **1998**, *275−277*, Pages 702.
(5) Matxain, J. M.; Fowler, J. E.; Ugalde, J. M. *Phys. Rev. A: At., Mol., Opt. Phys.* **2000**, *61*, 053201/1.
(6) Spano, E.; Hamad, S.; Catlow, C. R. A. *J. Phys. Chem. B* **2003**, *107*, 10337. Hamad, S. Personal communication.
(7) Spano, E.; Hamad, S.; Catlow, C. R. A. *Chem. Commun.* **2004**, *7*, 64.
(8) Muilu, J.; Pakkanen, T. A. *Surf. Sci.* **1996**, *364*, 439.
(9) Woodley, S. M.; Sokol, A. A.; Catlow, C. R. A. Z. *Anorg. Allg. Chem.* **2004**, *630*, 2343.
(10) Martin, T. P. *Phys. Rep.* **1996**, *273*, 199.
(11) Burnin, A.; BelBruno, J. J. *Chem. Phys. Lett.* **2002**, *362*, 341.
(12) Roberts, C.; Johnston, R. L. *Phys. Chem. Chem. Phys.* **2001**, *3*, 5024.
(13) Straatsma, T. P.; Apra, E.; Windus, T. L.; Dupuis, M.; Bylaska, E. J.; Jong, W. D.; Hirata, S.; Smith, D. M. A.; Hackler, M. T.; Pollack, L.; Harrison, R. J.; Nieplocha, J.; Tipparaju, V.; Krishnan, M.; Brown, E.; Cisneros, G.; Fann, G. I.; Fruchtl, H.; Garza, J.; Hirao, K.; Kendall, R.; Nichols, J. A.; Tsemekhman, K.; Valiev, M.; Wolinski, K.; Anchell, J.; Bernholdt, D.; Borowski, P.; Clark, T.; Clerc, D.; Dachsel, H.; Deegan, M.; Dyall, K.; Elwood, D.; Glendening, E.; Gutowski, M.; Hess, A.; Jaffe, J.; Johnson, B.; Ju, J.; Kobayashi, R.; Kutteh, R.; Lin, Z.; Littlefield, R.; Long, X.; Meng, B.; Nakajima, T.; Niu, S.; Rosing, M.; Sandrone, G.; Stave, M.; Taylor, H.; Thomas, G.; Lenthe, J. v.; Wong, A.; Zhang, Z. NWChem 4.5. Version 4.5 ed.; Pacific Northwest National Laboratory: Richland, WA, 2003; pp NWChem 4.5.
(14) Kohn, W.; Sham, L. J. *Phys. Rev.* **1965**, *140*, A1133−A1138.
(15) Becke, A. D. *J. Chem. Phys.* **1993**, *98*, 5648.
(16) Lee, C.; Yang, W.; Parr, R. G. *Phys. Rev. B: Condens. Matter Mater. Phys.* **1998**, *37*, 785.
(17) Krishnan, R.; Binkley, J. S.; Seeger, R.; Pople, J. A. *J. Chem. Phys.* **1980**, *72*, 650.
(18) McLean, A. D.; Chandler, G. S. *J. Chem. Phys.* **1980**, *72*, 5639.
(19) Wachters, A. J. H. *J. Chem. Phys.* **1970**, *52*, 1033.
(20) Hay, P. *J. Chem. Phys.* **1977**, *66*, 4377.

(21) Chem 3D Pro 8.0; 8.0 ed.; CambridgeSoft Corporation: Cambridge, England, 2004.

(22) Holden, N. E. Atomic masses and abundances. In *CRC Handbook of Chemistry and Physics*; 84th ed.; CRC Press: New York, 2002−2003; p 1.

(23) Echt, O.; Sattler, K.; Recknagel, E. *Phys. Rev. Lett.* **1981**, *47*, 1121.

(24) Kroto, H. W.; Heath, J. R.; O'Brien, S. C.; Curl, R. F.; Smalley, R. E. *Nature* **1985**, *318*, 162.

(25) Katakuse, I. Microclusters. In *Microclusters*; Sugano, S., Nishina, Y., Ohnishi, S., Eds.; Springer-Verlag: Berlin, 1987; Vol. 4; p 10.

(26) Iijima, S.; Ishihashi, T.; Ando, Y. *Nature (London)* **1992**, *356*, 776.

(27) Kroto, H. W. *Nature (London)* **1987**, *329*, 529.

(28) Jarrold, M. F. *Nature (London)* **2000**, *407*, 26.

(29) Harrison, W. A. *Electronic Structure and the Properties of Solids*; W. H.Freeman and Company: San Francisco, CA, 1980.

(30) Swank, R. K. *Phys. Rev.* **1967**, *153*, 844.

(31) Tillack, M. S.; Blair, D. W.; Harilal, S. S. *Nanotechnology* **2003**, *15*, 390.